Rock and Soil Mechanics

Volume 43 | Issue 1 Article 1

3-23-2022

On water migration and frost heaving characteristics of sand under water vapor recharge

Hua-yang LEI
Key Laboratory of Comprehensive Simulation of Engineering Earthquake and Urban-Rural Seismic Resilience, China Earthquake Administration, Tianjin 300350, China

Wen-zhen ZHANG
Department of Civil Engineering, Tianjin University, Tianjin 300354, China

Shuang-xi FENG
Key Laboratory of Comprehensive Simulation of Engineering Earthquake and Urban-Rural Seismic Resilience, China Earthquake Administration, Tianjin 300350, China, shuangxiyaokaoyan@163.com

Hai-feng HUO
School of Airport, Civil Aviation University of China, Tianjin 300300, China

Rock and Soil Mechanics 2022 43(1): 1−14 ISSN 1000−7598
https: //doi.org/10.16285/j.rsm.2021.6009 rocksoilmech.researchcommons.org/journal

On water migration and frost heaving characteristics of sand under water vapor recharge

LEI Hua-yang[1, 2, 3], ZHANG Wen-zhen[1], FENG Shuang-xi[1,3], HUO Hai-feng[4]

1. Department of Civil Engineering, Tianjin University, Tianjin 300354, China

2. Key Laboratory of Coast Civil Structure Safety of Ministryof Education, Tianjin University, Tianjin 300354, China

3. Key Laboratory of Comprehensive Simulation of Engineering Earthquake and Urban-Rural Seismic Resilience, China Earthquake Administration, Tianjin 300350, China

4. School of Airport, Civil Aviation University of China, Tianjin 300300, China

Abstract: The influences of different initial water contents, cold end temperatures and dry densities on water migration in sand were studied using the self-developed water migration and frost heaving testing equipment. The variations of frost heaving force and frost heaving amount subjected to aforementioned three factors were analyzed and the position of freezing front was determined. The results show that the initial water content and cold end temperature had significant influence on the soil water migration and frost heaving effect. When the initial water content increased from 0% to 10%, the peak water content increased by 6.00 times, the horizontal frost heaving force and frost heaving amount increased gradually, and the freezing front moved up to the position of 2.5 cm in height. When the cold end temperature decreased from −5 ℃ to −15 ℃, the peak water content increased by 4.38 times, the horizontal frost heaving force and frost heaving amount increased gradually, and the freezing front moved up to the position of 2.6 cm in height. Dry density has relatively insignificant influence on water migration and freezing characteristics of samples. Under low dry density, there was an overall trend of slightly larger increases in sample's water content, horizontal frost heaving force and frost heaving amount, and the position of freezing front was concentrated at the position of 2.2–2.5 cm in height. The prediction formulae of frost heaving force and frost heaving amount were put forward for different influencing factors, and they can provide a reference for understanding the water migration law in sand under water vapor recharge and reasonably preventing frost heave.

Keywords: sand; water migration; frost heaving characteristics; water vapor recharge

1 Introduction

Supported by national initiatives such as the 'the Belt and Road' and 'Building up a country with strong transportation network', construction of large-scale high-speed railways has been accelerated in China. According to the literature[1−4], 75% of the construction and operation of high-speed railways are located in seasonally frozen areas in China, such as Changchun−Jilin high-speed railway, Panjin−Yingkou high-speed railway and Zhengzhou−Xi'an high-speed railway. Coarse-grained fillers are widely used in the bottom layer of high-speed railway subgrade. However, under the combined effects of rainfall, groundwater and temperature, the subgrade heaving phenomenon induced by the frost heave of coarse-grained fillers has been encountered for several times in the existing high-speed railways in the seasonally frozen area[5]. It is found that water vapor caused by temperature gradients continues to converge to the cold end and changes its phase, which is the main cause for sand frost heave[6-7]. Therefore, it is of great significance to understand the water migration law and frost heaving characteristics of sandy soil under water vapor recharge, and to provide essential theoretical basis for reducing engineering accidents and ensuring the safe operation of railways.

The available researches on the changes in soil engineering properties caused by water vapor migration mainly focused on fine sand[8], silt[9] and clay[10]. The temperature gradient, initial water content, dry density and other factors are considered to be the major factors that affect water migration law. For example, Joshua et al.[11] pointed out that at the longitudinal temperature gradient, the water in the fine sand mainly migrates from the high temperature end to the low temperature end in the form of water vapor. When the water vapor condenses into liquid water, it will move from the low temperature end to the high temperature end under the action of the temperature gradient. Dobchuk et al.[12] found through experiments that dry density, porosity and diffusion coefficient are the major factors affecting the gaseous water migration in silt. Wang et al.[13] believed that sandy silt has a

Received: 6 July 2021 Revised: 3 November 2021
This work was supported by the National Key Research and Development Program (2017YFC0805402), the Open Fund Project of the State Key Laboratory of Civil Engineering Disaster Prevention (SLDRCE17-01) and the National Natural Science Foundation of China (52078334).
First author: LEI Hua-yang, female, born in 1974, PhD, Professor, PhD supervisor, focusing on geotechnical engineering. E-mail: 15620559771@163.com
Corresponding author: FENG Shuang-xi, male, born in 1988, Postdoctor, Assistant Research Fellow, focusing on geotechnical engineering. E-mail: shuangxiyaokaoyan@163.com

critical water content. When the water content is too large or too small, the amount of water migration is insignificant. Li et al.[14] carried out the migration experiments on mixed gaseous and liquid water under different temperature gradients and proposed that the amount of gaseous and liquid water migration is proportional to the temperature gradient, and the increase in the amount of gaseous water migration is greater than that of liquid water migration. Through analysis, it is found that in the literature, although some researches have been conducted on the water migration of frozen soil, most of them focused on the combined action of liquid and gaseous water, and there are few results on the influence of gaseous water recharge on the water and gas migration law of coarse-grained soils. Studies have shown that the coarse-grained soil is greatly affected by water vapor recharge, and the gaseous water migration can cause obvious frost heaving deformation of the sample[15].

Frost heaving force and frost heaving amount are the important indicators for evaluating soil frost damage. Frost heaving force has important theoretical significance for revealing the interaction mechanism between frozen soil and structure. Research on frost heaving force (horizontal, normal and tangential frost heaving forces) focuses on two aspects: theoretical calculation and experimental analysis[16]. For example, Zhang et al.[17] found that the maximum horizontal frost heaving force from the top to the bottom of the loess sample showed a trend of first increasing and then decreasing, and the maximum value appeared at the relative height of the sample from 0.6 to 0.8. Gao et al.[18] proposed a contact model of normal and tangential frost heaving forces for U-shaped trenches, and verified the correctness of the contact model through experiments and numerical simulations. In addition, the study of the frost heaving amount focused on the influences of the fine particle content, mineral composition and salt content on the frost heaving characteristics of the soil. For example, Zhang et al.[19] believed that the fine particle content has insignificant effect on the freezing depth of coarse-grained fillers. Lin[20] studied the influence of clay minerals on the frost heave of silty clay and believed that part of the frost heave of the sample with 20% montmorillonite content was contributed by the film water migration, and the remaining frost heave was mainly attributed to the in situ freezing of water in the soil. Wu et al.[21] conducted research on the frost heaving characteristics of fine silt with high salt content and found that the frost heave of salty silt is less affected by the water content but mainly depends on the salt content. Through analysis, one can find that there is little research on the change law of frost heaving force and frost heaving amount of soil under water vapor recharge, and the evaluation of frost heaving force and frost heaving amount is relatively scarce.

In this paper, the B_3 group filler (medium sand) of the high-speed railway subgrade is studied. The freezing test is carried out through the self-developed water migration and frost heaving testing equipment. The effects of cold end temperature (characterizing temperature gradient), dry density and initial water content on the sand water migration law and frost heaving characteristics under water vapor recharge are analyzed. The variations of temperature, water content and frost heave of samples under different influencing factors are obtained, and the position of freezing front (the interface between frozen area and unfrozen area) is determined. The empirical relationship between the frost heaving amount and horizontal frost heaving force is proposed. It provides a reference for the follow-up theory and engineering application.

2 Testing setup and program

2.1 Testing sample

The sandy soil used in the test was sampled from a certain section of the Dandong−Dalian high-speed railway subgrade. The basic physico-mechanical parameters of the sandy soil are listed in Table 1.

Table 1 Basic physico-mechanical properties of testing soil

Natural density /(g • cm^{-3})	Specific gravity of soil	Permeability coefficient /(cm • s^{-1})	Compression modulus /MPa	Particle distribution /%		
				0.5−2.0 mm	0.25−0.50 mm	0.075−0.250 mm
1.76	2.66	5.3×10^{-2}	44	26.2	54.6	19.2

2.2 Testing device

In this paper, the water migration and frost heaving testing equipment is developed, as shown in Fig.1. The equipment consists of a refrigerating device, a model barrel, a monitoring system and a sampling system. Its working principle is shown in Fig.2. The compressor, condenser, solenoid valve, copper tube and capillary copper tube are connected to form a miniature refrigerating device. The capillary copper tube is tightly packed in two layers inside the freezer box to enhance the cooling effect. The freezer box is covered with a plastic film and placed beneath the sample as the cold end, and the gap between the freezer box and the barrel wall is blocked with an insulating gel to isolate the outside water and temperature. The model barrel is made of plexiglass with dimensions of 15 cm×10 cm×1 cm (height×inner diameter×thickness), and the outside is wrapped with thermal insulation glue to reduce the

exchange of energy between the sample and the environment. Fine holes are drilled every 2.0 cm along the height to install sensors to monitor the temperature and pressure of the sample.

2.3 Monitoring system and sensor calibration

The monitoring system includes temperature, pressure and displacement monitoring.

2.3.1 Temperature monitoring

The PT100 temperature sensor with size of ϕ4 mm× 30 mm and accuracy of level A is inserted into the sand sample. The temperature monitoring range of the sensor is −200−260 ℃, and the accuracy is ±0.15 ℃. It is connected with a temperature indicator (CH702 digital display intelligent temperature controller), and it can monitor and record temperature changes in real time.

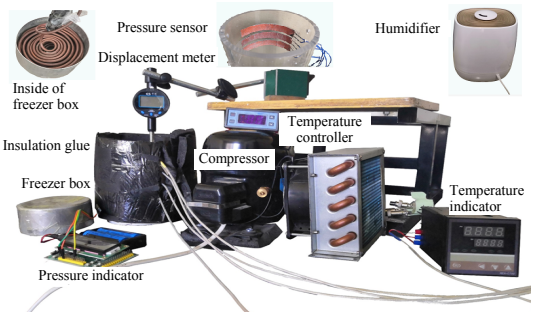

Fig. 1 Self-developed water migration and frost heaving testing equipment

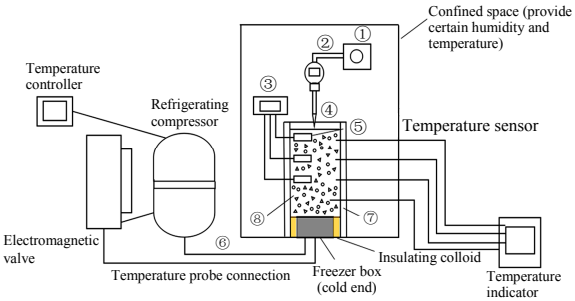

① Magnetic base ② Displacement meter ③ Earth pressure indicator ④ Model barrel (upper part is not covered) ⑤ Earth pressure sensor ⑥ Thermally conductive copper tube ⑦ Insulation gel ⑧ Specimen

Fig. 2 Schematic diagram of temperature controlling equipment

2.3.2 Cold end temperature control

During the freezing process, the temperature of the bottom plate is controlled by the temperature probe provided by the refrigerating equipment, and the temperature control probe is embedded at the position 0.5 cm above the contact surface between the aluminum box and the sand. At the temperature setting stage, the cold end temperature is preset first. When the temperature of the sample recorded by the probe is higher than the preset temperature, the compressor will continue to work. When the sample temperature recorded by the probe reaches the preset value, the compressor will stop working. When the temperature rises, the compressor will continue to work. The time for it starts and stops is about 4 min. Its cold end temperature error is always controlled within 2 ℃, as shown in Fig.3.

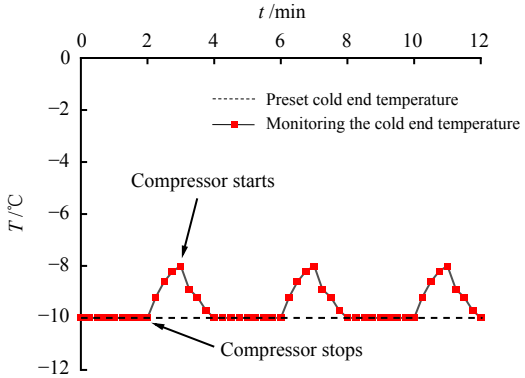

Fig. 3 Schematic diagram of cold end temperature control (−10 ℃)

2.3.3 Horizontal frost heaving force monitoring

To monitor the change of horizontal frost heaving force in real time, the RP-L flexible film pressure sensor is attached to the inner wall of the model and connected with a pressure indicator (the pressure indicator is composed of 51 single-chip microcomputer and LCD1602 display screen). The pressure sensing range is 20 g−10 kg, and the resolution is ±5%. The sensor is calibrated by comparing the mass of the weight with the displayed value after applying a weight of 20−100 g (at a loading interval of 20 g), as shown in Fig.4. It can be seen that the mass of the weight is consistent with the displayed value, which can meet the requirements of measurement accuracy.

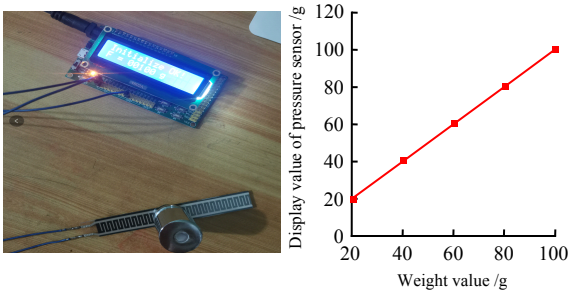

(a) Photo of pressure calibration (b) Relationship between display value of pressure sensor and weight value

Fig. 4 Calibration of pressure sensor

2.3.4 Frost heaving amount monitoring

A duralumin sheet with a diameter of 0.5 cm and a thickness of 0.2 mm is placed in the center of the upper surface of the sample, and the frost heaving amount of the sample is measured by an electronic displacement meter (SHSIWI digital dial indicator). The displacement measurement range of the displacement meter is 0−10 mm, and the accuracy is 0.001 mm.

2.3.5 Indoor temperature and humidity control

The indoor temperature is maintained at 20 ℃ using the air conditioner, and the temperature range changes within ±3% recorded by the thermometer. The indoor humidity is maintained at 70% by means of the humidifier. The hygrometer is placed next to the model barrel, and manually adjusted every 2 h to control the humidity error within ±5%. During the test, the upper part of the sample is exposed to the laboratory environment, in order to ensure that water vapor can effectively recharge the sample.

2.4 Testing schemes

The surface temperature of the sampling area is −5 ℃ to −15 ℃ in winter, and the temperature of the underground normal temperature layer is about 20 ℃. Therefore, the air conditioner in the laboratory is used to keep the temperature of the upper part of the sample constant at 20 ℃ (humidification end temperature). The humidifier is adopted to control the indoor humidity at 70%, and the cooling device is employed to maintain the temperature of the lower end of the sample at −5 ℃, −10 ℃ and −15 ℃, respectively (cold end temperature). Thus the temperature gradient of the subgrade filler under water vapor recharge in seasonally frozen area in the natural conditions is simulated.

Let the maximum dry density of the sample be 1.60 g/cm^3, and the optimal water content be 10%. Following the "*Code for design of railway earth structure*" (TB 10001－2016)[22], the B_3 group of medium sand is selected as the filler. The samples with different initial water contents (0%, 5%, 10%) and different initial dry densities (1.60, 1.55, 1.50, 1.45, 1.40 g/cm^3) are prepared in the laboratory, in order to compare the influences of cold end temperature, initial water content and dry density on the water vapor migration law and frost heaving characteristics. The testing schemes are listed in Table 2, and seven parallel tests are done each time for each working condition.

Table 2 Experimental schemes

Working condition	Cold end temperature /℃	Humidification end temperature /℃	Initial water content w_0/%	Dry density ρ_d/(g • cm^{-3})	Testing time t/d
1	−10	20	0	1.50	1−7
2	−10	20	5	1.50	1−7
3	−10	20	10	1.50	1−7
4	−10	20	5	1.40	1−7
5	−10	20	5	1.45	1−7
6	−10	20	5	1.55	1−7
7	−10	20	5	1.60	1−7
8	−5	20	5	1.50	1−7
9	−15	20	5	1.50	1−7

2.5 Testing procedure

The test includes several key steps such as sample preparation and installation, setting of warm end temperature and measurement of water content, frost heaving force and frost heaving amount after freezing treatment.

(1) The freezer box is installed at the bottom of the model barrel and then sealed. Pressure sensors are arranged at the heights of the model barrel at s = 2.0, 4.0, 6.0, 8.0 and 10.0 cm, respectively. The layered compaction method is used to prepare a cylindrical sample with size of 10 cm×10 cm (height×diameter). The sample is prepared as follows: divide the sample into three equal parts by mass and divide the model barrel along the height into three equal parts and mark the scale line. Considering the impact of vibrating the upper soil on the compactness of the lower soil, the lower and middle soils should be slightly higher than the scale line of the model barrel after compaction, the surface soil should be disturbed by scratches and the soil should be continued to fill in the upper part, to ensure the uniformity of the soil. A temperature sensor is arranged in the prefabricated hole of the model cylinder and then sealed.

(2) An electronic displacement meter is installed on the top of the sample to measure the frost heaving amount. Before the compressor starts to work, the displacement meter is set to zero. In an insulated laboratory, the indoor temperature and humidity are set to 20 ℃ and 70%, respectively. The bottom of the sample is cooled down through a micro-refrigeration system, and the controller sets the temperature at the bottom of the sample to −5 ℃, −10 ℃ and −15 ℃, respectively.

(3) During freezing process, the temperature, horizontal frost heaving force and frost heaving amount are monitored. Once the test starts, the aforementioned test data are registered every 1 h. When the temperature of the sample at each hole position becomes stable, the interval of saving data is adjusted to 8 h. The frequency of saving data for frost heaving force and frost heaving amount is the same as that of temperature. For the same working condition, seven samples are used to measure the water content. One sample is dismantled every day, and two soil samples are obtained at every 1.0−2.0 cm along the height. The water contents of the two soil samples are measured by the drying method. The arithmetic mean is taken as the final water content of the sample at this height.

3 Analysis of test results

3.1 Variation law of temperature field

Taking working conditions 2, 8 and 9 for example, the variations of temperature for the samples under different cold end temperatures with time are investigated, as shown in Fig.5. It can be seen that the sample temperature increases from the bottom to the top. As the freezing time increases, the top temperature decreases. The greater the temperature gradient (or the lower the cold end temperature), the higher the zero-degree Celsius line of the temperature field, and the longer it

takes for the field to stabilize. One can see from Fig.5(a) (working condition 8) that the temperature field of the sample is not stable after 1 d of freezing, and the temperature of the upper part (at the heights of 5.0−10.0 cm) is 20 ℃. After 2 d of freezing, the temperature field at the lower part of the sample (at the heights of 1.0−5.0 cm) is basically stable, the temperature at the heights of 8.0−10.0 cm is maintained at 20 ℃, and the temperature difference between the cold end and humidification end reaches about 25 ℃. It can be seen from Figs.5(b) and 5(c) (working conditions 2 and 9) that the temperature field in the lower part of the sample tends to be stable after 2−3 d of freezing, and the upper part temperature is lower than 20 ℃. After 7 d of freezing in the three working conditions, the temperature field has reached a basically stable state, and the temperature of the lower end of the sample (at a height of 0 cm) is approximately close to the preset cold end temperature.

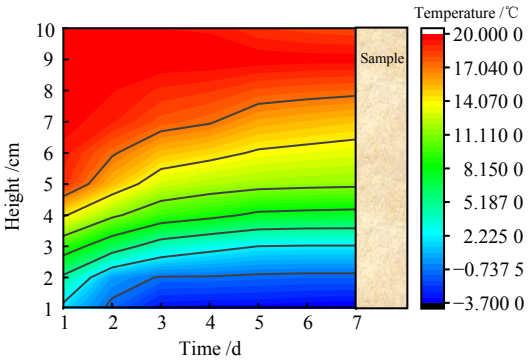

(a) Working condition 8 with cold end temperature of −5 ℃

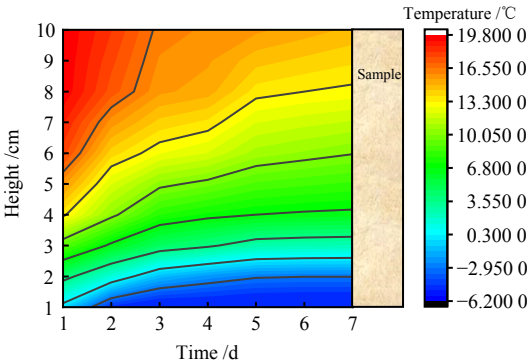

(b) Working condition 2 with cold end temperature of −10 ℃

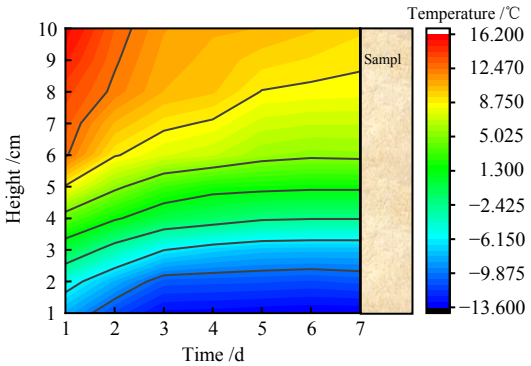

(c) Working condition 9 with cold end temperature of −15 ℃

Fig. 5 Temperature distribution under different cold end temperatures

3.2 Water migration law

3.2.1 Influence of altitude

Taking working condition 9 for example, the variations of water content of the samples at different heights s with time are investigated, as shown in Fig.6. It can be seen that the warm end is located at s = 10.0 cm, and the water content is basically unchanged. As the height of the sample decreases, the water content continues to increase, reaching the highest at s = 2.0 cm. The water content increases with the increase in freezing time, by 27.5% at the most. This shows that under the action of low temperature, the external water vapor migrates to and gathers at the position of s = 2.0 cm.

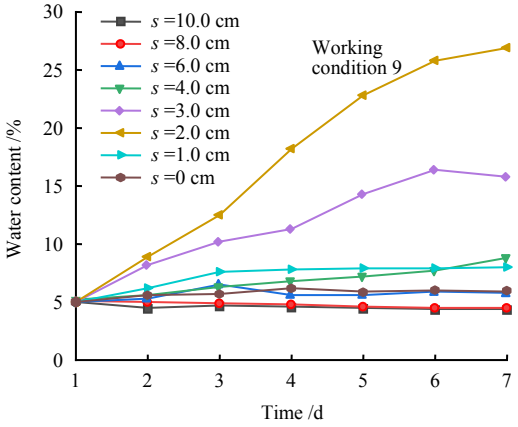

Fig. 6 Variation curves of water content at different heights

Under water vapor recharge, part of the water vapor will condense into the liquid phase. At this time, gaseous water and liquid water migrate to the cold end simultaneously and freeze into ice at the cold end. The test results show that it is easy to produce ice lens at the height of 2.0−3.0 cm from the cold end (Fig.7), where water will accumulate and transform into ice. It will block the migration of water to the cold end, thus the water content changes little after the ice lens is formed at the heights of 0−1.0 cm. The continuous formation of ice increases the suction and promotes the migration of water to the ice lens. At the same time as it thickens, more crushed ice will be produced on the upper part. It can be seen that the water content at a height of 3.0 cm is relatively larger; in other upper positions, the increase in water content is slight.

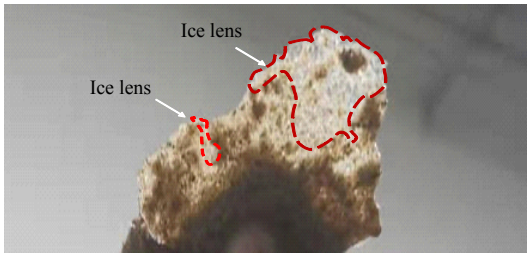

Fig. 7 Ice lens generated

3.2.2 Influence of cold end temperature

Taking working conditions 2, 8 and 9 for example, the variations of water content for the samples under different cold end temperatures with time are investigated, as shown in Fig.8. It can be seen that as the freezing time increases, the peak water content gradually increases, and the water migration phenomenon becomes more obvious. After 3 d of freezing, the peak water contents of the samples all appear under the three working conditions. After the peak water content, the water content of the samples below the peak position (near the cold end) basically stagnates with time. This is because an ice lens is formed near the position with peak water content, which prevents the water vapor in the soil from migrating downward and causes the water to continue to accumulate, which aggravates the rapid increase of the peak water content to a certain extent.

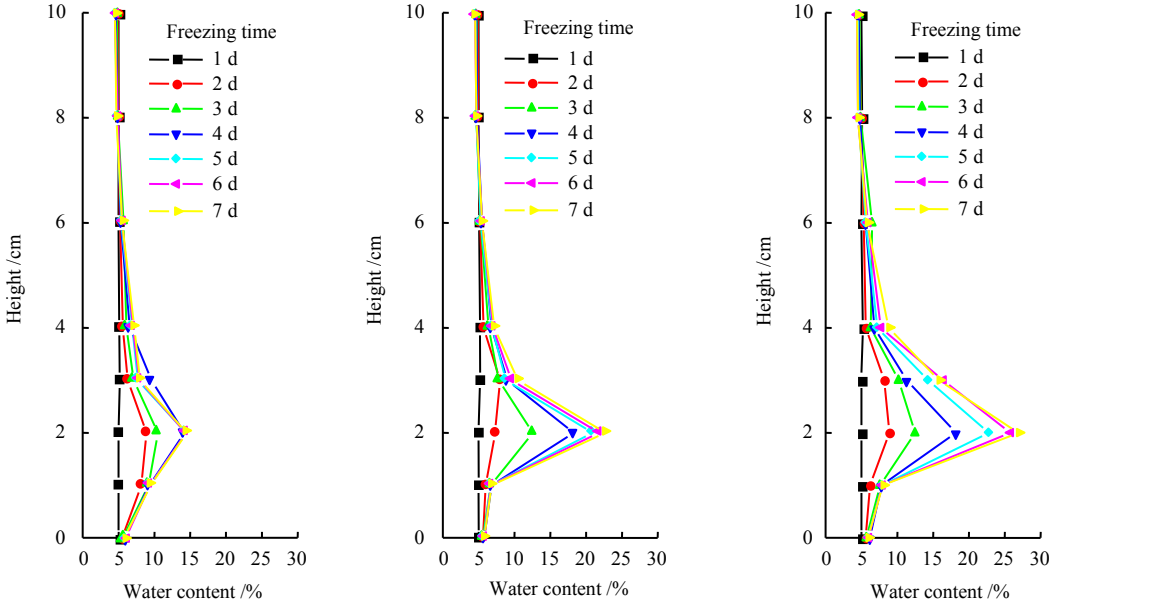

(a) Working condition 8 with cold end temperature of −5 ℃ (b) Working condition 2 with cold end temperature of −10 ℃ (c) Working condition 9 with cold end temperature of −15 ℃

Fig. 8 Water migration law under different cold end temperatures

Figure 9 shows the distribution curves of water content of the sample under working conditions 2, 8 and 9 after 7 d of freezing. It can be seen that as the height of the sample increases, the water content shows a trend of first increasing and then decreasing. When the cold end temperature is −5 ℃ (condition 8), an obvious peak water content appears at a height about 1.0 cm from the cold end, which increases from 5.0% to 14.5%, by 1.9 times. When the cold end temperatures are −10 and −15 ℃, an obvious peak water content appears at a height about 2.0 cm from the cold end, and the water content increases from 5.0% to 22.7% and 26.9%, by 3.54 and 4.38 times, respectively. The tests show that as the cold end temperature decreases, the peak water content increases significantly, and the water vapor migration phenomenon becomes more obvious. This is because as the cold end temperature decreases, the sample absorbs more heat at the same time, and the internal temperature of the sample decreases rapidly, which accelerates the formation of ice, thereby increasing the suction and accelerating the rates of water migration and phase change. It can be seen from Fig.9 that the increase in water content is relatively large at the cold end temperature of −15 ℃.

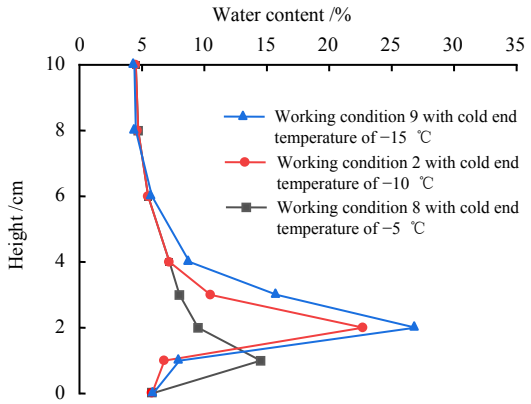

Fig. 9 Water content distribution curves under different cold end temperatures

3.2.3 Influence of initial water content

Taking working conditions 1, 2 and 3 for example, the variations of water content of samples at different initial water contents with freezing time are investigated, as shown in Fig.10. It can be seen that as the height of the sample increases, the water content first increases and then decreases. The sample with an initial water content of 0% has a peak at a height of 1.0 cm, and the peaks for samples with initial water contents of 5% and 10% are located at a height of 2.0 cm. The greater the initial water content, the larger the overall water

content of the sample after 7 d of freezing. When the initial water content of the sample is 0%, the peak water content at a height of 1.0 cm is about 5%. When the initial water content is 5%, the peak water content at a height of 2.0 cm is about 23%. When the initial water content is 10%, the water content at a height of 2.0 cm is about 30%. Compared with the samples with the initial water content of 0%, the peak water contents of the samples with the initial water contents of 5% and 10% increase by 3.6 and 5.0 times, respectively, showing that the gain of peak water content increases with the initial water content.

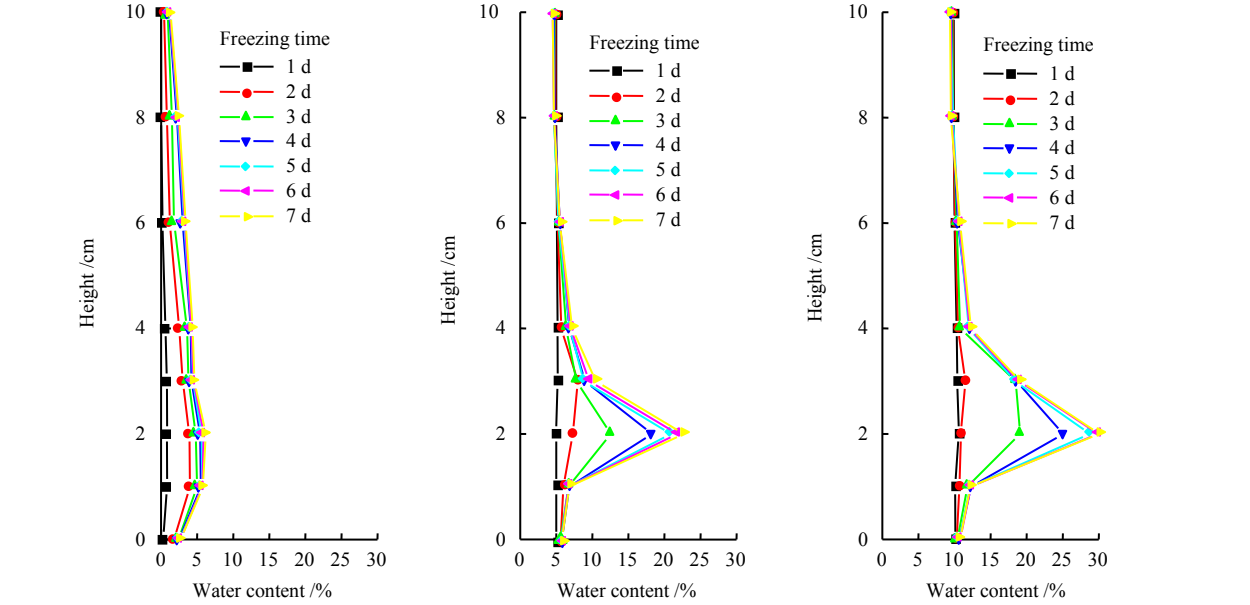

(a) Working condition 1 with initial water content of 0% (b) Working condition 2 with initial water content of 5% (c) Working condition 3 with initial water content of 10%

Fig. 10 Water migration law of samples with different initial water contents

Figure 11 shows the variation curves of water content at the height of 2.0 cm of the samples under working conditions 1, 2 and 3 with freezing time. It can be seen that as the freezing time increases, the water content curve shows a nonlinear increasing trend. At the initial water content w_0 of 0%, the water content of the sample reaches its peak after 2−3 d of freezing. The samples with initial water contents of 5% and 10% reach the peak water content at 4−6 d.

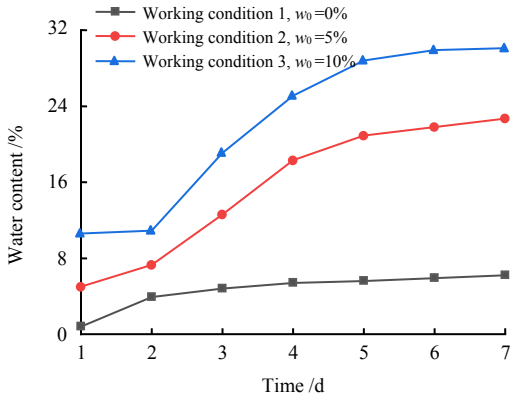

Fig. 11 Variation curves of water content at 2.0 cm height of soil sample with different initial water contents

3.2.4 Influence of dry density

Taking working conditions 2, 4, 5 and 7 for examples, the variations of water content for the samples at different dry densities with time are investigated, as shown in Fig.12. It can be seen that the samples under the four working conditions all reach the peak water contents after 2 d of freezing. The longer the freezing time, the greater the peak water content. The dry density of the sample increases from 1.40 g/cm^3 to 1.60 g/cm^3, and the peak water content is stabilized in the range of 22.5%−25.5% after 7 d of freezing.

Figure 13 shows the variation of water content versus height of samples under working conditions 2, 4, 5, 6 and 7 after 7 d of freezing. It can be seen that the variation trend of the water content of the samples with different dry densities is basically the same, and the peak water content appears at the height of 2.0 cm. The dry density has little effect on water vapor migration, but at lower dry densities, the water content of the sample increases slightly. This may be related to the porosity of the sample. Since the specific surface area of the coarse-grained soil is small, and the surface suction is lower than that of fine-grained soil, consequently, the larger porosity can provide a channel for water vapor recharge. Due to water suction of the coarse-grained soil lower than that of the fine-grained soil, its aeration and water flow capacity is higher, as a result, the water content increases more under small density. On the contrary, under the larger dry density, the smaller porosity is not conducive to the migration and recharge of water vapor.

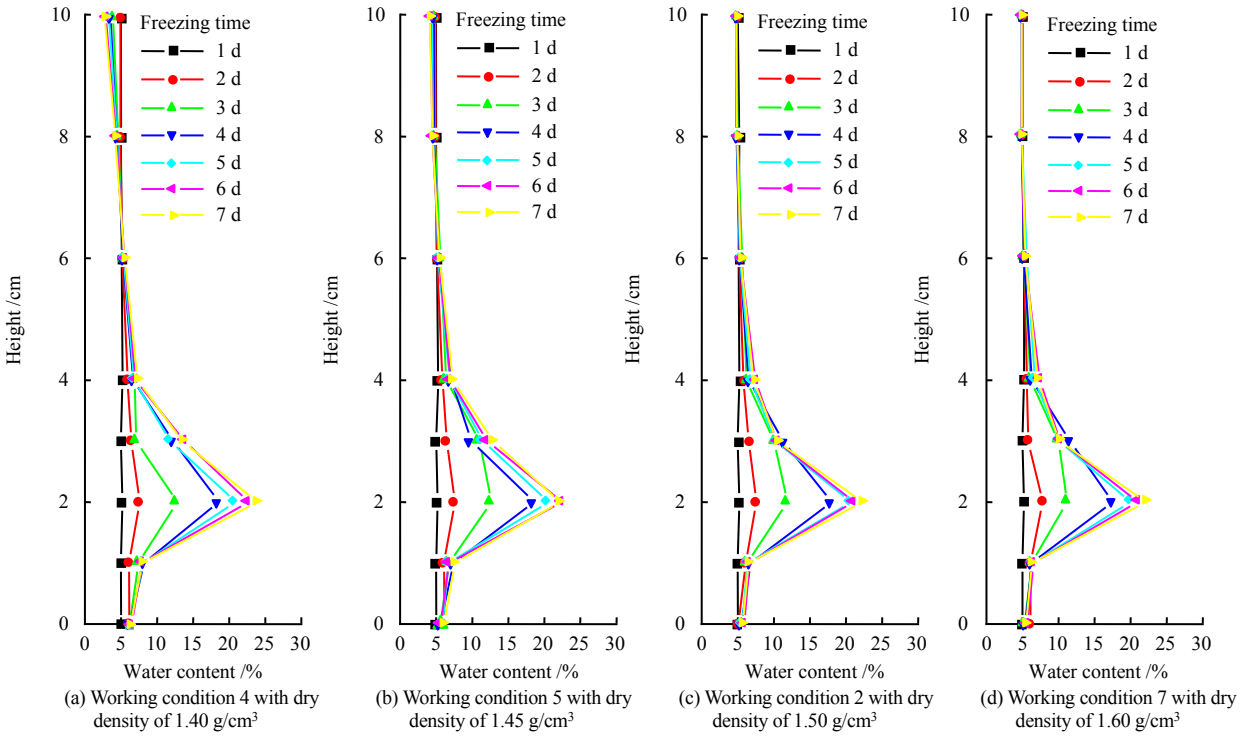

Fig. 12 Water migration law of samples with different dry densities

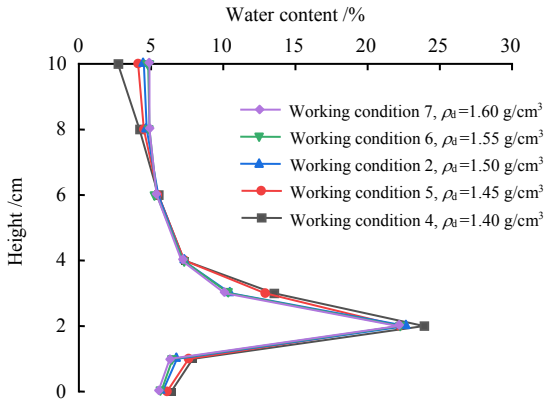

Fig. 13 Variation curves of water content of samples with different dry densities

Fig. 14 Photo of frozen soil at cold end

It can be seen from Figs.8, 10 and 12 that the water content of the lower part of the sample near the cold end increases significantly, and the water content of the upper warm end hardly changes with the freezing time. One can see from Fig.11 that when the initial water content is 0%, the water content at a height of 2.0 cm increases with the freezing time, and the water content reaches 6.2% after 7 d of freezing. Figure 14 shows the photo of the cold end of the sample after 7 d of freezing. This proves that the redistribution of water in the sample results from the water vapor migration and recharge in the environment.

3.3 Variation characteristics of horizontal frost heaving force

3.3.1 Influence of initial water content

The horizontal frost heaving force F is defined as the force of the soil on the boundary of the unit area in the horizontal direction during the frost heaving process[17]. Taking working conditions 1, 2 and 3 for instance, the variations of horizontal frost heaving force with freezing time t at different positions of samples with different initial water contents are shown in Fig.15. It can be seen that as the freezing time increases, the horizontal frost heaving force shows a gradual increase trend. The greater the initial water content, the larger the frost heaving force. At a height of 2.0 cm and after 7 d of freezing, the frost heaving forces of the samples with the initial water contents of 10% and 0% reach 5.94 kPa and 1.19 kPa, respectively (Fig.15(a)). At a height of 4.0 cm, the frost heaving forces of the samples with the initial water contents of 10% and 0% reach 5.05 kPa and 2.01 kPa, respectively (Fig.15(b)). At a height of 10.0 cm, the frost heave forces of the samples with the initial water contents of 10% and 0% reach 3.09 kPa and 1.19 kPa, respectively (Fig.15(c)). Soil freezing is essentially a coupled process

of heat and water migration. The horizontal frost heaving force depends on the amount of ice generated and is closely related to the temperature field. The ice contents of the samples with different initial water contents vary. On the one hand, as the initial water content increases, the specific heat capacity of the soil increases, and the stabilization speed of temperature field becomes slower under the same external environment. On the other hand, the thermal conductivity of the water is greater than that of the soil. When the initial water content increases, the thermal conductivity of the soil increases, and the stabilization speed of temperature field accelerates. The two contradictory factors restrict each other. From the test results, the increase in thermal conductivity has a greater impact on the temperature field and ice volume, i.e. the horizontal frost heaving force of the samples with high initial water content is large.

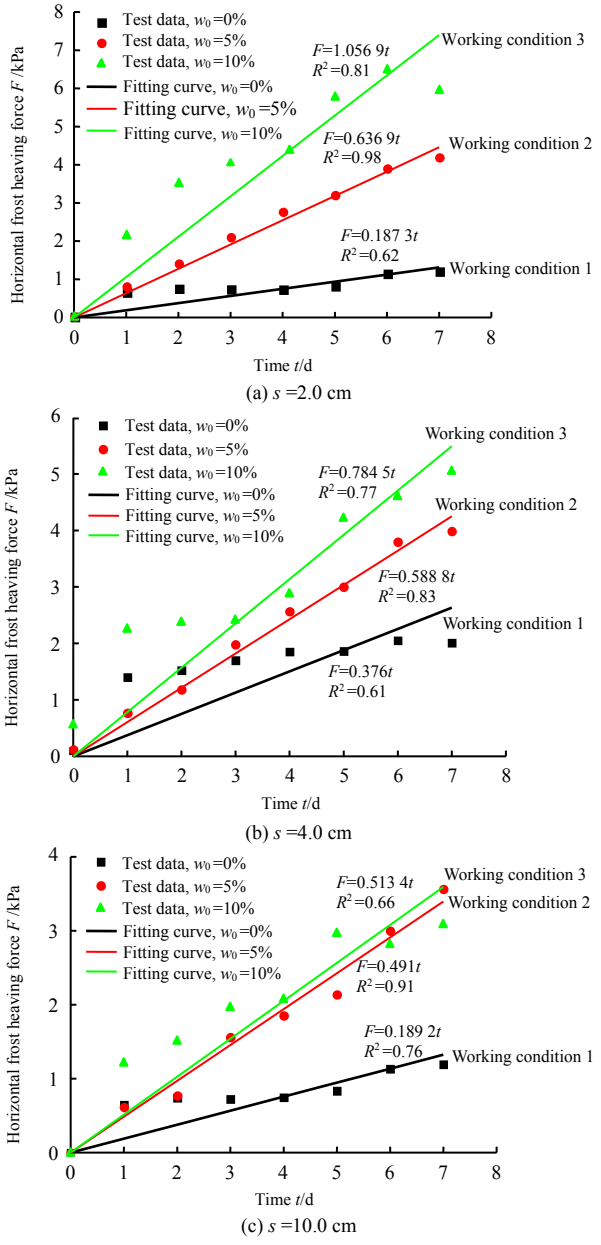

Fig. 15 Horizontal frost heaving force−time curves under different initial water contents

3.3.2 Influence of cold end temperature

Taking working conditions 2, 8 and 9 for instance, the variations of the horizontal frost heaving force for the samples under different cold end temperatures with the freezing time are shown in Fig.16. It can be seen that the lower the cold end temperature, the greater the horizontal frost heaving force after 7 d of freezing. At a height of 2.0 cm and after 7 d of freezing, the frost heaving forces of the samples at the cold end temperature of −5, −10 and −15 ℃ are 3.37, 4.25 and 4.50 kPa, respectively (Fig.16(a)). At a height of 4.0 cm, the horizontal frost heaving forces of the samples at the cold end temperature of −5, −10 and −15 ℃ are 2.36, 4.04 and 4.26 kPa, respectively (Fig.16(b)). At a height of 10.0 cm, the frost heaving forces of the samples

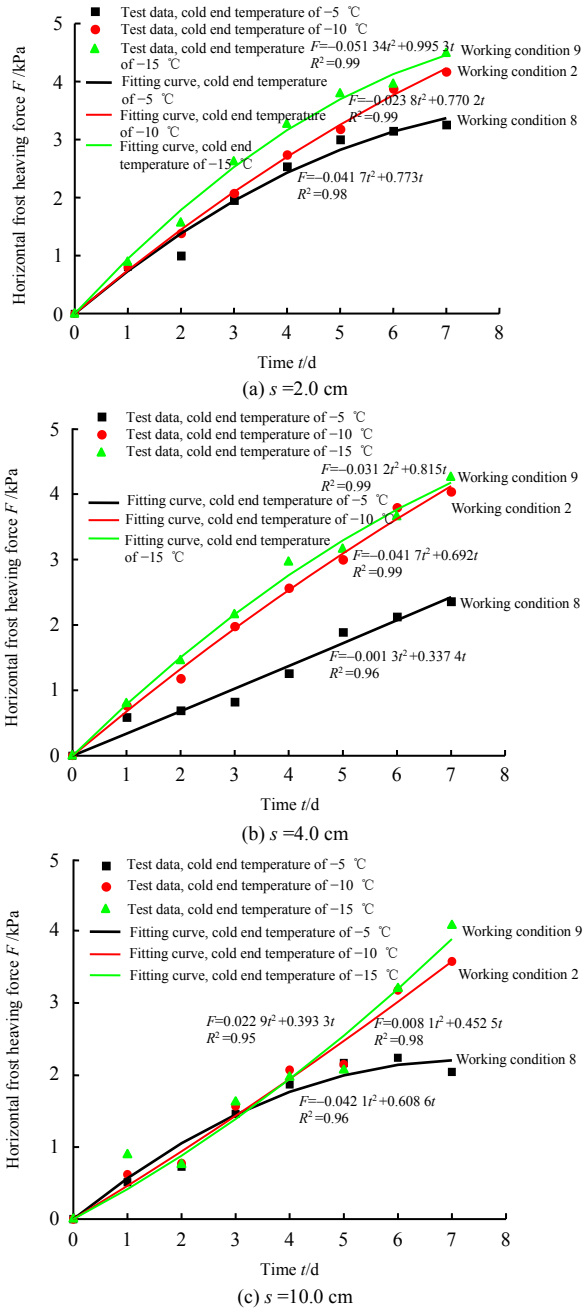

Fig. 16 Relation curves of cold end temperature with horizontal frost heaving force

at the cold end temperature of −5, −10 and −15 ℃ are 2.04, 3.56 and 4.06 kPa, respectively (Fig.16(c)). The lower the cold end temperature, the faster the freezing edge moves upwards, the greater the thickness of the freezing layer. The larger the entire freezing area, and the greater the ice lens content, resulting in the increases in the expansion of the sample and the frost heaving force.

3.3.3 Influence of dry density

Taking working conditions 2, 4, 5, 6 and 7 for instance, the variations of horizontal frost heaving force for the samples at different dry densities with freezing time are shown in Fig.17. By fitting the relationship between the horizontal frost heaving force and the freezing time, it can be seen that when the dry density increases from 1.40 g/cm^3 to 1.60 g/cm^3, the variation ranges of frost heaving force at the heights of 2.0, 4.0 and 10.0 cm are [0.55t, 0.75t], [0.51t, 0.72t] and [0.28t, 0.63t], respectively. As the dry density increases, the frost heaving force of the sample decreases, because migrated gaseous water is the only recharge source during the freezing process of the sample. The water is mainly transferred through the pores of the sample. The sample with high dry density has lower porosity, thus there are fewer channels and higher resistance for water migration, and at the same time, less ice and lower frost heaving force are generated. Considering engineering practice, increasing the dry density of subgrade filling can hinder the phenomenon of water vapor migration to a certain extent, and effectively reduce the horizontal frost heaving force of subgrade.

3.4 Variation characteristics of frost heaving amount

3.4.1 Influence of initial water content

Taking working conditions 1, 2 and 3 for instance, the changes of frost heaving amount for the samples at different initial water contents with freezing time are shown in Fig.18(a). It can be seen that for the same freezing time, the greater the initial water content, the larger the frost heaving amount of the sample. When the initial water content is 10%, the frost heaving amount reaches 3.50 mm after 7 d of freezing. When the initial water content is 0%, the frost heaving amount is 0.42 mm after 7 d of freezing, and it is reduced by 88.0%. The frost heaving amount of the sample is closely related to the degree of water phase change. The sample with high initial water content has more water to freeze in situ and has a large thermal conductivity, and thus it is easy to form a freezing edge and then form an ice lens. The formation of ice lens accelerates the adsorption of water, resulting in a larger frost heaving amount for samples with high water content.

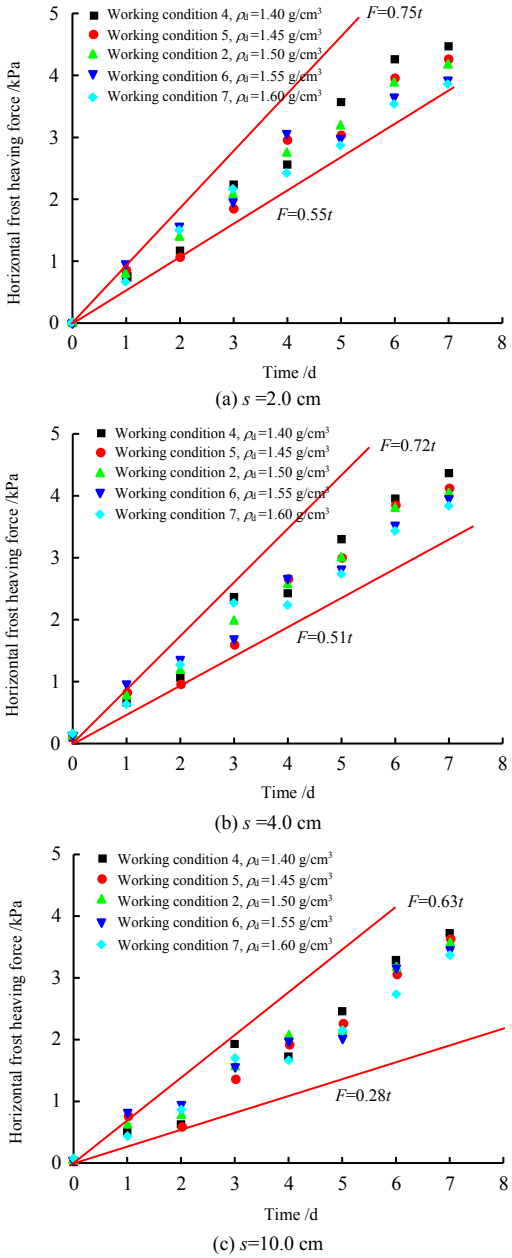

Fig. 17 Relation curves of dry density with horizontal frost heaving force

In order to describe the influence of different water contents on the frost heaving amount, firstly, the linear fitting method is used to obtain the empirical relationship between the frost heaving amount and time (Fig.18(a)):

$$V = at \quad (1)$$

where V is the frost heaving amount; and a is the fitting coefficient.

The relationship between the fitting coefficient a and the initial water content w_0 is shown in Fig.18(b). Thus the empirical formula for the initial water content w_0 and frost heaving amount V is

$$V = (0.003\ 1w_0^2 + 0.010\ 5w_0 + 0.069\ 6)t \quad (2)$$

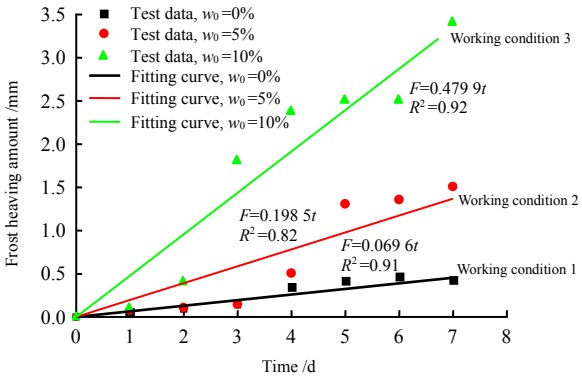

(a) Relationship between frost heaving amount and time

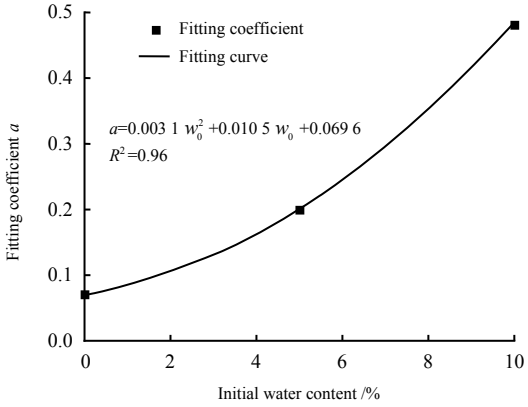

(b) Relationship between fitting coefficient and initial water content

Fig. 18 Relation curve of initial water content with frost heaving amount

3.4.2 Influence of cold end temperature

Taking working conditions 2, 8 and 9 for example, the changes of frost heaving amount of the samples under different cold end temperatures with freezing time are shown in Fig.19. It can be seen that for the same freezing time, the lower the cold end temperature of the sample, the greater the frost heaving amount. After 7 d of freezing, when the cold end temperature is −15 ℃, the frost heaving amount is 3.41 mm; and when the cold end temperature is −5 ℃, the frost heaving amount is 0.44 mm. In combination with the characteristics of the curve, the relationship between the frost heaving amount and time is fitted, as shown in Fig.19(a). Then, the relationship between the fitting coefficient and the cold end temperature is shown in Fig.19(b). Hence, the empirical expression for the cold end temperature T with the frost heaving amount V is

$$V=(-0.036\ 3T-0.138\ 8)t \tag{3}$$

3.4.3 Influence of dry density

Taking working conditions 2, 4, 5, 6 and 7 for instance, the changes of frost heaving amount for the samples with different dry densities with freezing time are shown in Fig.20. It can be seen that for the same freezing time, the lower the dry density of the sample, the greater the frost heaving amount. When the dry density is 1.40 g/cm^3 after 7 d of freezing, the frost heaving amount reaches 2.78 mm. When the dry density

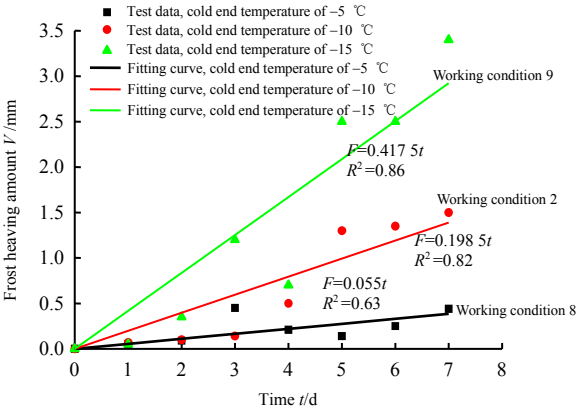

(a) Relationship between frost heaving amount and time

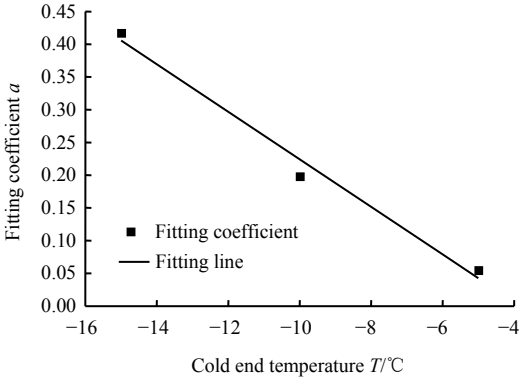

(b) Relationship between fitting coefficient and temperature

Fig. 19 Relation curve of cold end temperature with frost heaving amount

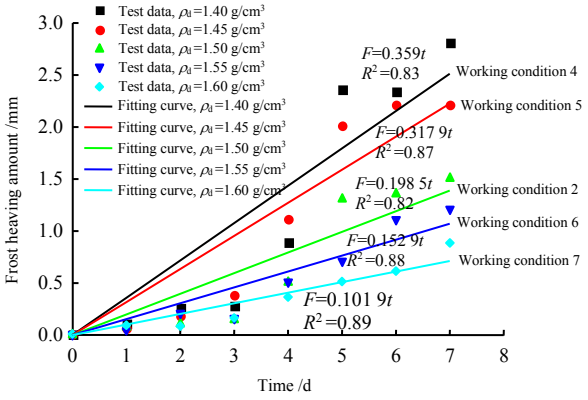

(a) Relationship between frost heaving amount and time

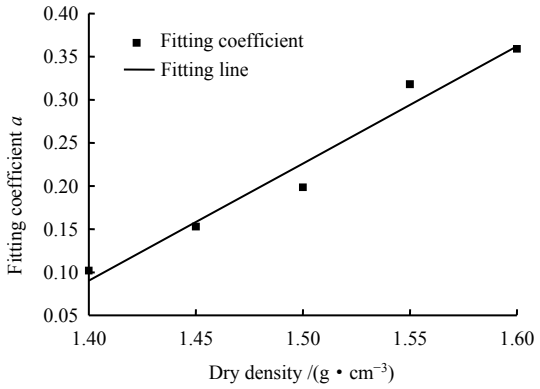

(b) Relationship between fitting coefficient and dry density

Fig. 20 Relation curves of dry density with frost heaving amount

is 1.60 g/cm^3, the frost heaving amount is 0.87 mm, with a reduction of 68.71%. Similarly, combining Figs.20(a) and 20(b), we can establish the empirical expression between frost heaving amount and dry density as

$$V=(1.358\ 4\rho_{\mathrm{d}}-1.811\ 6)t \tag{4}$$

3.5 Variation law of freezing front position

The interface between the frozen area and the unfrozen area is the freezing front. Understanding its variation rule is helpful to determine the location of the frost heaving boundary of sand (Fig.21(a)) and guide engineering design and construction. The working condition 2 is selected to study the variations of the positions of the zero-degree Celsius line and the freezing front. It can be seen from Fig.21(b) that the positions of the zero-degree Celsius line and the freezing front gradually move up with the increase in freezing time, but the freezing front position is always below the zero-degree Celsius line, i.e. the freezing front is closer to the cold end of the sample. As the freezing time increases, the temperature of the sample tends to stabilize, and the zero-degree Celsius line is located at a height of 2.5 cm. A freezing front appears when the sample is frozen for 3 d, and the freezing front is located at a height of 2.3 cm when it is frozen for 7 d. As the freezing time increases, in the area between the warm end of the ice lens and the freezing front, ice particles begin to grow and gradually connect.

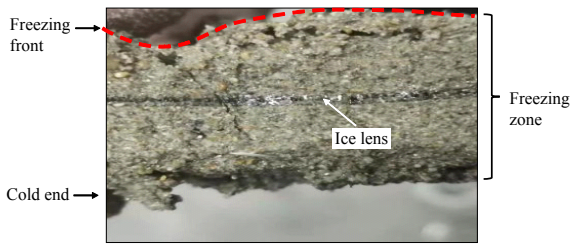

(a) Freezing front

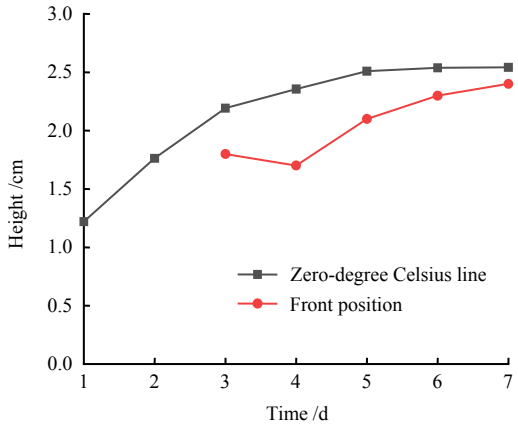

(b) Evolution curves of zero-degree Celsius line and freezing front for working condition 2

Fig. 21 Positions of zero-degree Celsius line and freezing front

The unfrozen water content and permeability coefficient gradually decrease, and it becomes more and more difficult for water to migrate to the warm edge of the ice lens. The freezing front becomes more and more difficult to move toward the zero-degree Celsius line, and finally stabilizes in the equilibrium position.

The working conditions 2 and 3 are selected to study the change of initial water content on freezing front position. The working conditions 2, 8 and 9 are selected to study the change of cold end temperature on freezing front position. The working conditions 2, 4, 5, 6 and 7 are selected to investigate the effect of dry density on the position of freezing front, as shown in Fig.22.

It can be seen from Fig.22(a) that for the same freezing time, the greater the initial water content, the higher the freezing front of the sample. After 7 d of freezing, the sample with an initial water content of 0% has no freezing front; for a sample with an initial water content of 5%, the freezing front is located at a height of 2.4 cm; and for a sample with an initial water content of 10%, the freezing front is located at a height of 2.5 cm. Compared to the sample with the initial water content of 5%, the sample with the initial water content of 10% has a higher proportion of liquid water. The freezing front is formed first, and its position moves up first under the action of water vapor migration, resulting in a higher position of freezing front.

It can be seen from Fig.22(b) that the position of freezing front shows an upward trend as the cold end temperature decreases. After 7 d of freezing, for the sample with cold end temperature of −15 ℃, the freezing front is located at a height of 2.6 cm. For the sample with cold end temperature of −5 ℃, the freezing front is located at a height of 1.8 cm. This is because with the same thermal conductivity, as the freezing time increases, the position of the zero-degree Celsius line of the sample with a low cold end temperature is higher than that of the sample with a high cold end temperature, and the position of freezing front moves along the zero-degree Celsius line.

It can be seen from Fig.22(c) that the position of freezing front of the sample at the early freezing stage does not change significantly with the dry density. The position of freezing front at the late freezing stage shows an upward trend with the increase of dry density, and it is concentrated at the heights of 2.2−2.5 cm after 7 d of freezing. As the freezing time increases, the migration of water vapor continues to add water to the freezing edge of the sample, the freezing edge gradually thickens and the position of freezing front gradually moves up. Until the cold end temperature is reached, overlying pressure, ice pressure and water

flow are in equilibrium state, and the ascending rate of the freezing front position is stable.

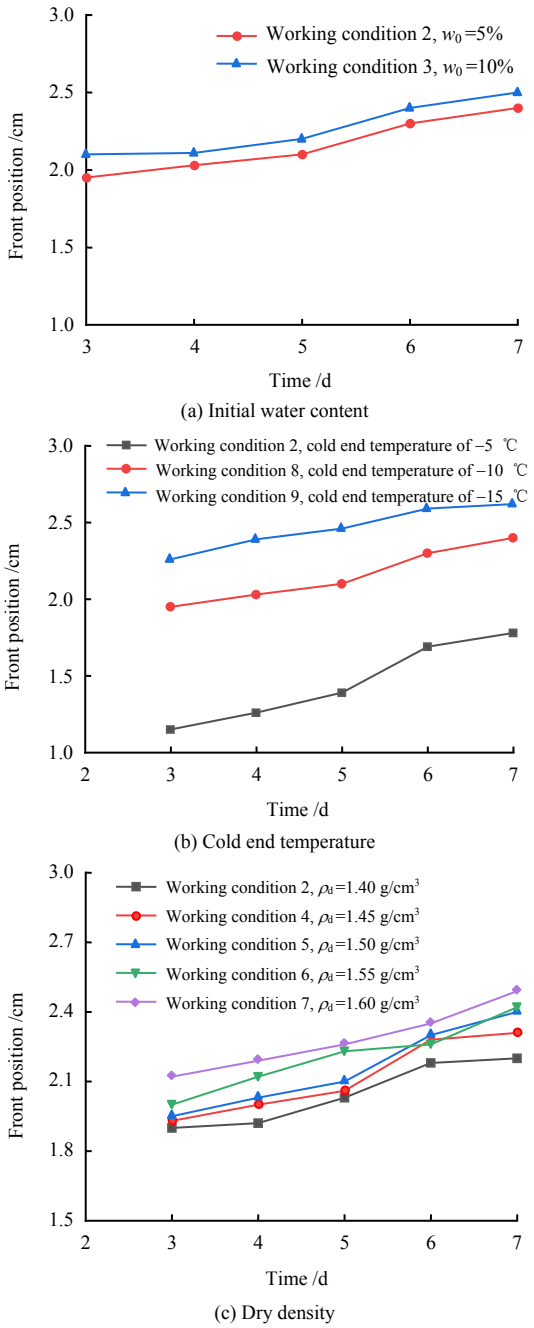

Fig. 22 Relation curves of different factors with the position of freezing front

4 Conclusions

Using self-developed water migration and frost heaving testing equipment, the influences of initial water content, cold end temperature and dry density on sand water migration and frost heaving characteristics are studied. Following conclusions are drawn:

(1) The initial water content has significant influence on the water migration law and frost heaving characteristics of the sample. Compared to the sample with an initial water content of 0%, the peak water contents of the sample with initial water contents of 5% and 10% at a height of 2.0 cm increase by 4.6 and 6.0 times, respectively. The horizontal frost heaving force and frost heaving amount increase gradually, and the position of freezing front moves up to a height of 2.5 cm. Under high water content, the water inside the sample is more likely to turn into ice. More water will be adsorbed to migrate to the ice lens, and the phase change will continue to occur, resulting in a rapid increase in water content.

(2) The lower the cold end temperature, the higher the peak water content of the sample, and the greater the horizontal frost heaving force and frost heaving amount. When the cold end temperature is −5 ℃ after 7 d of freezing, the peak water content appears at a height of 1.0 cm, and it increases by 1.9 times. When the cold end temperatures are −10 and −15 ℃ after 7 d of freezing, the peak water content appears at a height of 2.0 cm, and the increments are 3.54 and 4.38 times, respectively. Compared with the sample with the cold end temperature of −5 ℃, the horizontal frost heaving force and frost heaving amount of the sample with the cold end temperature of −15 ℃ both increase, and the position of freezing front moves up to a height of 2.6 cm. With the decrease in cold end temperature, the internal temperature of the sample decreases rapidly, which accelerates the formation of ice phase and significantly increase the rate of water migration and phase change.

(3) Compared to the initial water content and cold end temperature, the dry density has relatively little influence on the water migration and frost heaving characteristics of the sample. The overall trend is that the water content, horizontal frost heaving force and frost heaving amount increase slightly. After 7 d of freezing, the peak water content is stable in the range of 22.5−25.5%, and the freezing front is concentrated at the height range of 2.2−2.5 cm.

A 7-d freezing test is carried out in this paper. The long-term freezing characteristics of sand under water vapor recharge need to be further explored by experiments. Under the combined recharge of water vapor and capillary water, the proportion of each contribution to frost heave needs to be explored.

References

[1] WANG Miao, MENG Shang-jiu, YUAN Xiao-ming, et al. Research on freezing-thawing correction coefficients of shear strength parameters of seasonal frozen soil[J]. Chinese Journal of Rock Mechanics and Engineering, 2018, 37(Suppl. 1): 3756−3764.

[2] SHEN Yu-peng, WANG Du-li, LIN Yuan-rong, et al. On the effect of prevention measures against horizontal frost heave of foundation pits over winter[J]. Rock and Soil

Mechanics, 2021, 42(5): 1434−1442.

[3] WU X Y, NIU F J, LIN Z J, et al. Delamination frost heave in embankment of high speed railway in high altitude and seasonal frozen region[J]. Cold Regions Science and Technology, 2018, 153: 25−32.

[4] CAI Han-cheng, MENG Jin-bao, ZHAO Xiang-qiang, et al. Design method of the thermosyphon embankment in permafrost region based on principle of heat balance[J]. Rock and Soil Mechanics, 2020, 41(11): 3769−3776.

[5] YANG You-hai, SHEN Xin, ZHU Sheng-xian, et al. Experimental study on frost heaving of coarse-grained filling material for Lanzhou−Xinjiang high speed railway[J]. China Railway Science, 2018, 39(3): 1−7.

[6] SONG Hong-fang, YUE Zu-run, LI Bai-lin, et al. Thermal insulation and strengthening properties of anti-frost heaving subgrade structure of the high-speed railway in seasonally frozen soil region[J]. Rock and Soil Mechanics, 2019, 40(10): 4041−4048.

[7] HE Zuo-yue, ZHANG Sheng, TENG Ji-dong, et al. Vapour transfer and its effects on water content in freezing soils[J]. Chinese Journal of Geotechnical Engineering, 2018, 40(7): 1190−1197.

[8] SHARMA R S, MOHAMED M H A. An experimental investigation of LNAPL migration in an unsaturated/ saturated sand[J]. Engineering Geology, 2003, 70(3-4): 305−313.

[9] TANG T, SHEN Y, LIU X, et al. The effect of horizontal freezing on the characteristics of water migration and matric suction in unsaturated silt[J]. Engineering Geology, 2021, 288: 106166.

[10] ZHANG Ru-ru, ZHAO Yun, XU Wen-jie, et al. Water-gas migration analysis in runway subgrade soil under influence of temperature[J]. Journal of Zhejiang University (Engineering Science), 2017, 50(5): 822−830.

[11] JOSHUA W D, JONG E D. Soil moisture movement under temperature gradients[J]. Canadian Journal of Soil Science, 1973, 53(1): 49−57.

[12] DOBCHUK B S, BARBOUR S L, ZHOU J. Prediction of water vapor movement through waste rock[J]. Journal of Geotechnical and Geoenvironmental Engineering, 2004, 130(3): 293−302.

[13] WANG Tie-xing, HE Zai-qiu, ZHAO Shu-de, et al. Experimental study on vaporous water transference in loess and sandy soil[J]. Chinese Journal of Rock Mechanics and Engineering, 2005, 24(18): 3271−3275.

[14] LI Yan-long, WANG Jun, WANG Tie-xing. Moisture migration of unsaturated soil due to thermal gradients[J]. Rock and Soil Mechanics, 2016, 37(10): 2839−2844.

[15] LIU Jian-long, TENG Ji-dong, ZHANG Sheng, et al. Experimental study on frost heave in unsaturated coarse-grained soil caused by vapour transfer[J]. Chinese Journal of Geotechnical Engineering, 2021, 43(7): 1297−1305.

[16] CUI Hong-huan, WANG Wei-hao, YAN Zi-lin, et al. Experimental study on frost heaving characteristics of railway subgrade in seasonal frozen area[J]. Journal of China and Foreign Highway, 2021, 41(1): 21−25.

[17] ZHANG Zheng, MA Xue-ning, ZHU Qi-you. Experimental analysis of horizontal frost heaving force of loess in Lanzhou City of Gansu Province Area[J]. The Chinese Journal of Geological Hazard and Control, 2021, 32(1): 102−107.

[18] GAO Feng, LOU Zong-ke, XIAO Min. Numerical simulation of frost heave damage of U-shaped canal considering interaction between concrete lining board and soil[J]. Journal of Yangtze River Scientific Research Institute, 2020, 37(1): 161−165.

[19] ZHANG Yu-zhi, WANG Tian-liang, ZHANG Fei, et al. Water vapor migration characteristics and frost heave characteristics of coarse-grained filler in high-speed railway subgrade under different fine particle contents[J]. China Railway Science, 2021, 42(4): 1−8.

[20] LIN Chao. Experimental study on the effect of clay minerals in silty clays on frost heave[D]. Xuzhou: China University of Mining and Technology, 2017.

[21] WU Ya-ping, PAN Gao-feng, LI Shuai, et al. Creep property of saturated fine sand with high salinity[J]. Journal of Highway and Transportation Research and Development, 2017, 34(7): 29−36.

[22] China Railway First Survey and Design Institute Group Co., Ltd. TB 10001−2016 Code for design of railway earth structure[S]. Beijing: China Railway Press, 2016.